AD-A083 554 NAVAL UNDERWATER SYSTEMS CENTER NEW LONDON CT NEW LO--ETC F/G 17/1
A NEARFIELD MODEL OF THE PARAMETRIC RADIATOR.(U)
DEC 75 R H MELLEN
UNCLASSIFIED NUSC-TM-PA4-230-75 NL

END
DATE FILMED
5-80
DTIC

AD A083554

TM No.
PA4-230-75

Naval Underwater Systems Center
New London Laboratory
New London, Connecticut 06320

Technical Memorandum

A NEARFIELD MODEL OF THE PARAMETRIC RADIATOR

Date: 31 December 1975

Prepared by: R. H. Mellen
Computer Sciences Department

APR 28 1980
A

TO BE PRESENTED AT THE 91ST MEETING OF THE
ACOUSTICAL SOCIETY OF AMERICA, WASHINGTON, DC,
APRIL 1976

Approved for public release;distribution unlimited.

DDC FILE COPY

80 4 28 010

LIST OF SYMBOLS

$S = \pi a^2$	=	Piston area
P_1, P_2	=	Primary pressures
P	=	Secondary (difference frequency) pressure
β	=	1 + B/2A nonlinearity number $\approx$ 3.6 for water
ρ_o	=	Normal density
c_o	=	Normal sound speed
k	=	Secondary wavenumber
k_o	=	Geometric mean primary wavenumber
R_o	=	Geometric mean primary Rayleigh distance
$\vec{r}$	=	Range (vector)
L	=	Range (scalar)
ϕ	=	Angle to field point
2α	=	$\alpha_1 + \alpha_2$ = Absorption (nepers/m)
x,t		Integration range variables
$2\alpha L$	=	Scaled range
$2\alpha R_o$	=	Absorption number
$2\alpha R_o\ k/k_o$	=	Nearfield absorption number
$2\alpha R_o\ k_o/k$	=	Farfield absorption number
k_o/k	=	Downshift ratio
W	=	Westervelt source level
Y	=	PL/W where PL is the apparent source level at L
z	=	u + jv complex variable
ϕ_w	=	$\sqrt{4\alpha/k}$ = Westervelt angle
θ	=	ϕ/ϕ_w

Reverse Blank

ABSTRACT

It is often necessary to measure and operate parametric radiators under conditions where finite range effects are important. A nearfield model is presented in which the source level is obtained by assuming the primary waves to be plane-cylindrical or diverging-conical depending upon whether the observation range is less or greater than the Rayleigh distance. Asymptotic beam patterns are obtained from the solution of an exponentially tapered line array. Nonlinear attenuation is not considered.

ADMINISTRATIVE INFORMATION

This memorandum was prepared under Project A-614-15, Subproject 11-121-706 Task 17442 "Parametric Echo Ranging Systems", Principal Investigator W. L. Konrad, Sponsoring activity NSSC SEA 06H1 J. Neely.

The author of this memorandum is located at the New London Laboratory, Naval Underwater Systems Center, New London, Connecticut 06320.

Reverse Blank

INTRODUCTION

In the Westervelt[1] model of the parametric radiator, an asymptotic approximation was made to obtain the source level and beam pattern at very long ranges. In many practical cases the conditions for this model are not met, therefore a finite-range model is essential.

Several methods[2-7] have been employed to obtain the field at finite range using various simplifying assumptions. In the present method the asymptotic beam pattern for points sufficiently far outside the primary beam is obtained from the solution for an infinite exponentially-tapered line array. The source levels are obtained by assuming the primary waves to be plane-cylindrical or diverging-conical depending on whether the observation point is less or greater than the Rayleigh distance. The other assumptions are that the absorption is linear and small compared to the secondary wave number.

Beam Patterns of a Line Array

For a parametric array the source strength per unit length is given by [1]

$$q(x,t) = \beta S \, \partial/\partial_t \, (P_1 P_2)/\rho_o^2 c_o^4 \qquad (1)$$

where $P_n = P_{on} \exp\left[-x(\alpha_n + ik_n) + i\omega_n t\right]$, $n = 1,2$

The difference frequency pressure for small S becomes

$$P(\vec{r},t) = -\rho_o \int_0^\infty dx \; q' \, (x, t - |\vec{r} - x|/c_o)/4\pi \, |\vec{r} - x| \qquad (2)$$

where q' indicates the time derivative

For $\vec{r} \to \infty$ Eq (2) gives the Westervelt result

$$rP(\emptyset) = \beta P_1 P_2 k^2 S/8\pi \rho_o c_o^2 \left[\alpha + ik \sin^2(\emptyset/2)^2\right] \qquad (3)$$

and $W = rP(0)$ is the Westervelt source level.

(The term $\exp(i\omega t - ikL)$ is omitted throughout.)

For finite range Eq. (2) can be written in terms of the dimensionless variable $Y = PL/W$ according to the geometry of Fig. 1 as

$$Y = 2\alpha L \exp(2\alpha L) \int_{-L}^{\infty} dx \frac{\exp\left[-2\alpha x - ik(\sqrt{x^2 + a^2} + x)\right]}{\sqrt{x^2 + a^2}} \qquad (4)$$

Eq. (4) can be rewritten as a contour integral

$$Y = 2\alpha L \exp(2\alpha L) \int_{z_0}^{\infty} \frac{dz \exp(-z)}{\sqrt{z^2 + B^2}}$$

where

$$z = 2\alpha x + ik(\sqrt{x^2 + a^2} + x) \qquad (5)$$

$$z_0 \approx -2\alpha L + ika^2/2L$$

$$B = 2a\,(\alpha^2 + ik\alpha)^{1/2}$$

and a typical contour is shown as the upper curve of figure 2.

Since $k/\alpha >> 1$ is the domain of interest the α^2 term in B will be neglected. Further, for small angles it is convenient to normalize $\phi \approx a/L$ to the Westervelt angle ϕ_w, hence,

$$z_0 = -u_0 + iv_0 \approx 2\alpha L(-1 + i\theta^2)$$

$$B^2 \approx 4i(2\alpha L\theta)^2 = 4iu_0v_0$$

where $\theta = \phi/\phi_w$.

Since the path of integration becomes rapidly oscillating for large z, the lower path of Fig. 2 where $v = v_0$ may be substituted to give the same result.

Changing variables to $z = t - u_0 + v_0$. Eq. (5) becomes

$$Y = 2\alpha L \exp(-iv_0) \int_{0}^{\infty} \frac{dt \exp(-t)}{\sqrt{(t - u_0)^2 - v_0^2 + 2iv_0(t + u_0)}} \qquad (6)$$

Eq. (6) was evaluated numerically and the results are shown in Figs. 3 and 4. Note that for the line source ($S \to 0$) there is a logarithmic singularity of strength $\exp(-2\alpha L)$ as $\theta \to 0$. Only for values of $2\alpha L \geq 10$ do patterns fall within 1 dB of the Westervelt asymptote. For smaller values of $2\alpha L$ the patterns tend to become narrower, approaching a minimum at $\theta = 1$ and increasing thereafter[6].

The line array patterns are asymptotic patterns of a parametric radiator at points sufficiently far outside the primary beams. For experimental comparison the axial level must be known. In order to determine the axial level it is necessary to account for the finite cross-section specifically.

CYLINDRICAL SOURCE

For a plane wave cylindrical source of radius a and the field point on the axis we have

$$P = \frac{\beta P_1 P_2 k^2 \exp(2\alpha L)}{4\pi \rho_o c_o^2} \int_{-L}^{\infty} dx \int_0^a da \, \frac{2\pi a \exp[-2\alpha x - ik(\sqrt{x^2 + a^2} + x]}{\sqrt{x^2 + a^2}} \qquad (7)$$

Integrating over a we have

$$P = \frac{\beta P_1 P_2 k}{i\, 2\rho_o c_o^2} \exp(2\alpha L) \left[\int_{-L}^{0} dx \exp(-2\alpha x) + \int_0^{\infty} dx \exp(-2\alpha x - 2ikx) \right.$$

$$\left. + \int_{-L}^{\infty} dx \exp(-2\alpha x + ik(\sqrt{x^2 + a^2} + x) \right] \qquad (8)$$

The second integral is omitted since $k \gg \alpha$ and its contribution negligible. Taking $z_2 = 2\alpha x + ik(\sqrt{x^2 + a^2} + x)$ in the third integral and neglecting terms in a^2 we obtain

$$4\alpha x = z - \sqrt{z^2 + B^2}$$

from which

$$4\alpha dx = dz \left[1 - \frac{z}{\sqrt{z^2 + B^2}} \right]$$

Substitution of the modified contour $z = t - u_o + iv_o$ in the third integral gives finally

$$Y_o = \frac{1}{iv_o}\left[\int_0^{u_o} dt\, \exp(-t)\right.$$

$$\left. - \frac{1}{2}\exp(-iv_o)\int_0^{\infty} dt\, \exp(-t)\left(1 - \frac{t - u_o + iv_o}{\sqrt{(t-u_o)^2 - v_o^2 + 2iv_o(t+u_o)}}\right)\right] \quad (9)$$

where $v_o = ka^2/2L \approx 2\alpha R_o\, k/k_o\, u_o$.

Eq. (9) was evaluated as a discontinuous function at $t = u_o$, since the integral converges more rapidly than by integrating the terms separately.

The results shown in Fig. 5 give the apparent source level as a function of scaled distance referred to the Westervelt source level at infinity. The parameter is the nearfield absorption number. Oscillations occur as the source level vs range changes from square-law to a slower rate. For all values of the parameter the asymptotic approach for the Westervelt limit is from above. This effect has a simple geometric explanation, i.e., the distance is measured from the origin rather than the "center of gravity" of the array, hence apparent source levels tend to be higher.

Note that the effects of absorption are negligible for $2\alpha L < 0.1$. From $2\alpha L = 0.1$ to 1 absorption begins to have an effect and for $2\alpha L > 1$ The curves approach the Westervelt limit. The resulting curves are asymptotic for $L \ll R_o$.

CONICAL SOURCE

For $L \gg R_o$ consider a conical source of spherically diverging primary waves and field point on the axis. Eq. (7) becomes

$$P = \frac{P_1 P_2 k^2 R_o^2}{2\rho_o c_o^2}\int_0^{\theta_o} d\theta \sin\theta \int_0^{\infty} dr\, \frac{e^{-[2\alpha r + ik(\sqrt{r^2 + L^2 - 2Lr\cos\theta} + r - L)]}}{\sqrt{r^2 + L^2 - 2Lr\cos\theta}} \quad (10)$$

Integrating over θ we obtain

$$P = \frac{P_1 P_2 k R_o^2 \theta_o^2}{i 2 \rho_o c_o^2 L}\left[\int_0^L dr\, \frac{\exp(-2\alpha r)}{r} + \int_L^\infty \frac{dr\, \exp[-2\alpha r - 2ik(r - L)]}{r}\right.$$

$$\left. - \int_0^\infty dr\, \frac{\exp[-2\alpha r - ik(\sqrt{r^2 + L^2 - 2Lr\cos\theta_o} + r - L)]}{r}\right] \qquad (11)$$

The second integral is again omitted. Substituting z for x in the third integral as in the cylindrical case and taking the new contour we have after some manipulation

$$Y = \frac{u_o}{iv_o}\left[\text{Res.} + \int_0^{u_o} dt\, \frac{\exp(-t)}{t}\right.$$

$$\left. - \int_0^\infty dt\, \frac{\exp(-t)}{t + u_o + iv_o}\, \frac{1 - \dfrac{t - u_o + iv_o}{\sqrt{(t - u_o)^2 - v_o^2 + 2iv_o(t + u_o)}}}{1 - \dfrac{t + u_o + iv_o}{\sqrt{(t - u_o)^2 - v_o^2 + 2iv_o(t + u_o)}}}\right] \qquad (12)$$

where $v_o = k L \theta_o^2/2$ ~~α~~ $u_o/(2\alpha R_o k_o/k)$ and Res. is the residue at z_o.

Although each integral has a pole at t = 0, the sum is well-behaved. Near zero the last integrand of Eq. (11) behaves as 1/z, where $z' = (1 + iv_o/u_o)t$ and it is necessary to evaluate the residue between the two paths. Take the contour from $z' = (1 + iv_o/u_o)\epsilon$ to $z' = (1 + i0)\epsilon$ and let $\epsilon \to 0$, which gives

$$\int_C \frac{dz'}{z'} = -\frac{1}{2} \ln\left[1 + (v_o/u_o)^2\right] - i \tan^{-1}(v_o/u_o)$$

Using the residue as the initial value, Eq. (12) was integrated as before and the results are shown in Fig. 6. The parameter in this case is the farfield absorption number. For values greater than 1, the approach to the asymptotic is again from above. For values less than 1, the asymptotic source levels fall below the Westervelt asymptotic and approach the asymptotic from below. This is the farfield diffraction effect where the generation becomes spherical and the source level approaches the exponential integral rather than the Westervelt asymptote[8].

COMPARISON WITH EXPERIMENT

Figure 7 shows the predicted source levels vs range compared to experimental results[5]. The downshift ratio was 7 and the value of $2\alpha R_0$ was 0.0175. The cylindrical and conical curves intersect near the Rayleigh distance. Above this point agreement with the conical curve is excellent while below the deviations are significant.

Figure 8 shows a comparison of experimental and predicted source levels vs range for a downshift of 50 with $2\alpha R_0 = 0.17$. Experimental values are approximately 3 dB low near the Rayleigh distance.

Figure 9 presents beam patterns of the second example made at two different distances: $2\alpha L = 0.25$ and 1. In the first case the experimental, rather than predicted axial value was used.

CONCLUSIONS

Predictions based on the nearfield model appear to be in fair agreement with experiment, however, further comparisons must be made to determine all the conditions for validity since errors can be large near the Rayleigh distance. The particular problem of nonlinear attenuation must also be included if the model is useful in a practical sense.[8] In its present form, however, it serves to illustrate the various finite range phenomenon of an absorption limited parametric radiator.

REFERENCES

1. P. J. Westervelt, "Parametric Acoustic Array", J. Acoust. Soc. Am 35, 535-537 (1963).

2. H. O. Berktay, "Nearfield Effects in Parametric End-fire Arrays" J. Sound. Vib. 20, 135-143 (1972).

3. J. G. Willette, "Difference Frequency Parametric Array Using an Exact Description of the Primary Sound Field", J. Acoust. Soc. Am. 52, 123(A) (1972).

4. T. G. Muir and J. G. Willette, "Parametric Acoustic Transmitting Arrays", J. Acoust. Soc. Am. 52, 1481-1486 (1972).

5. R. L. Rolleigh, "Difference Frequency Pressure Within the Interaction Region of a Parametric Array", J. Acoust. Soc. Am. 58, 964-971 (1975).

6. M. Vestrheim and H. Hobaek, "Angular Distribution of Nonlinearly Generated Difference Frequency Sound", Proceedings of a Symposium on Nonlinear Acoustics, Birmingham, England, March 1971.

7. H. Hobaek and M. Vestrheim, "Axial Distribution of Difference Frequency Sound in a Collimated Beam of Circular Cross Section", Proceedings of a Symposium on Nonlinear Acoustics, Birmingham, England, April 1971.

8. R. H. Mellen and M. B. Moffett, "A Model for Parametric Radiator Design", JUA 22, 2, 105-116 (UNCLASSIFIED) (April 1972).

FIGURE CAPTIONS

Figure 1 Geometry of Line Source

Figure 2 Contour Integration Paths. Branch points lie outside both paths and are not involved.

Figure 3 Beam Patterns. θ is the angle referred to the Westervelt angle and the parameter is the scaled distance $2\alpha L$ = 10 to 1

Figure 4 Beam patterns $2\alpha L$ = 1 to .01

Figure 5 Source level relative to Westervelt vs scaled distance. The parameter is the nearfield absorption number (plane wave model).

Figure 6 Source level relative to Westervelt vs scaled distance. The parameter is the farfield absorption number (spherical wave model).

Figure 7 Comparison of predicted and experimental values of apparent source level vs range $2\alpha R_o$ = 0.0175, k_o/k = 7

Figure 8 Comparison of predicted and experimental values of apparent source level vs range $2\alpha R_o$ = 0.17, k_o/k = 50.

Figure 9 Comparison of predicted and experimental beam patterns $2\alpha L$ = 0.25 and 1, k_o/k = 50.

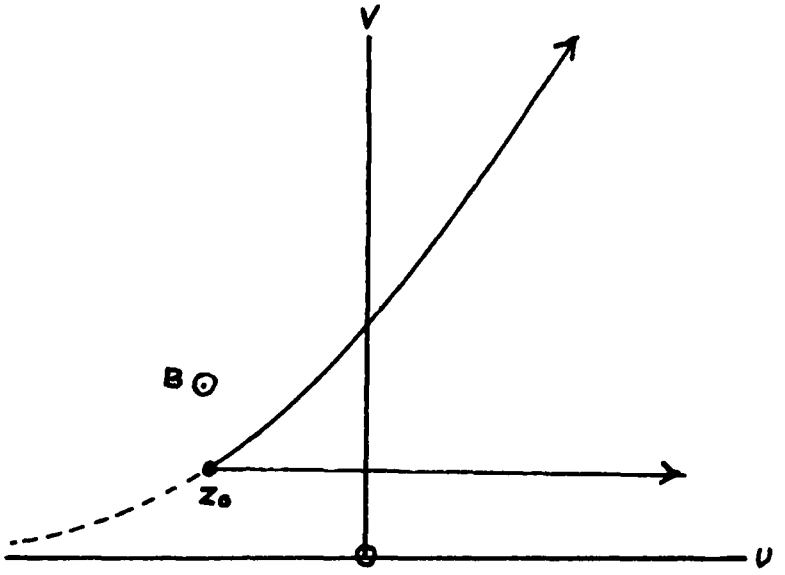

Fig. 2 - Contour Integration Paths

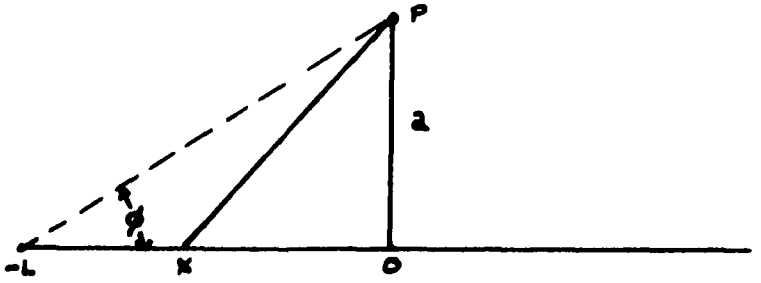

Fig. 1 - Geometry of Line Source

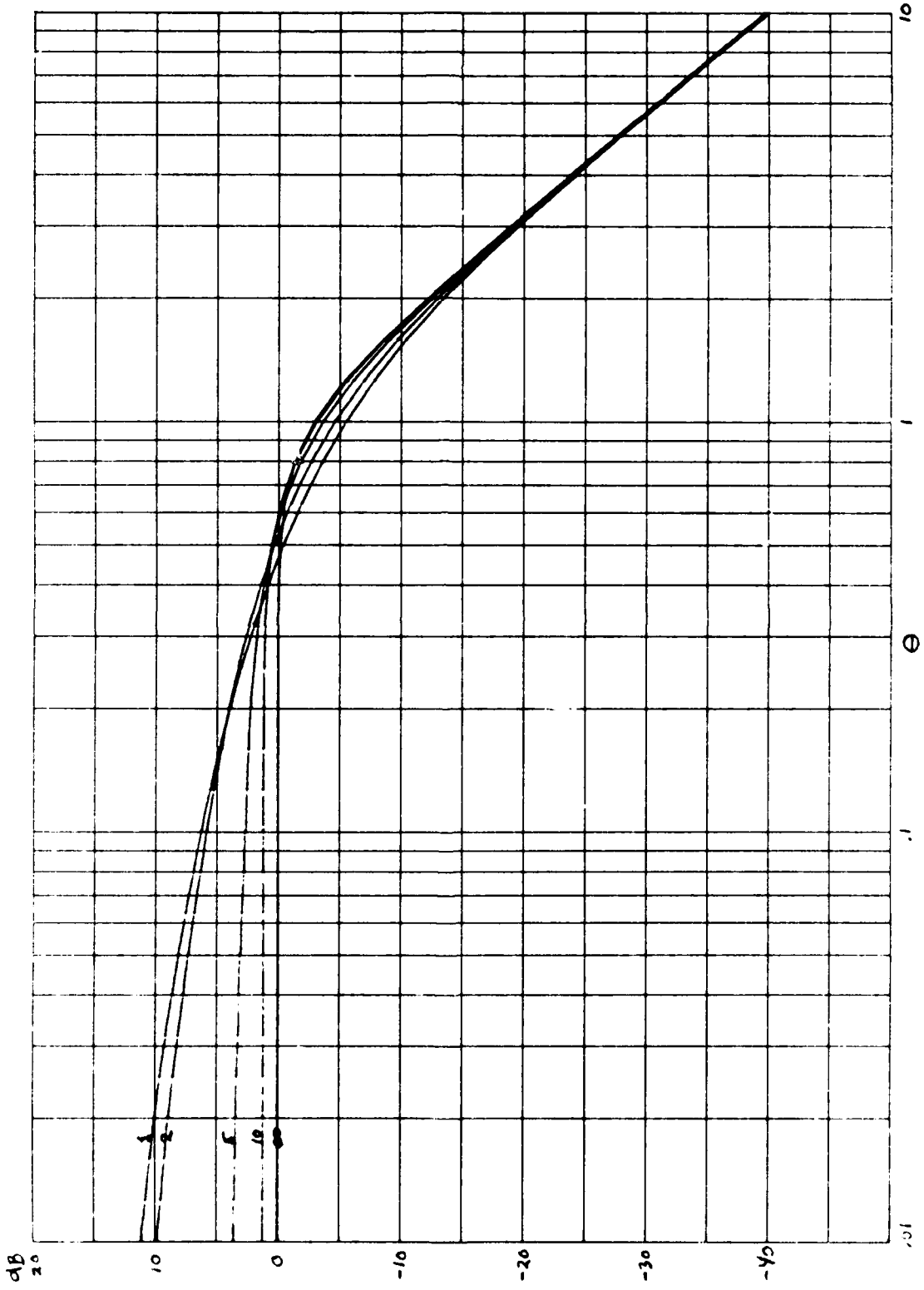

Fig. 2 - Beam Patterns

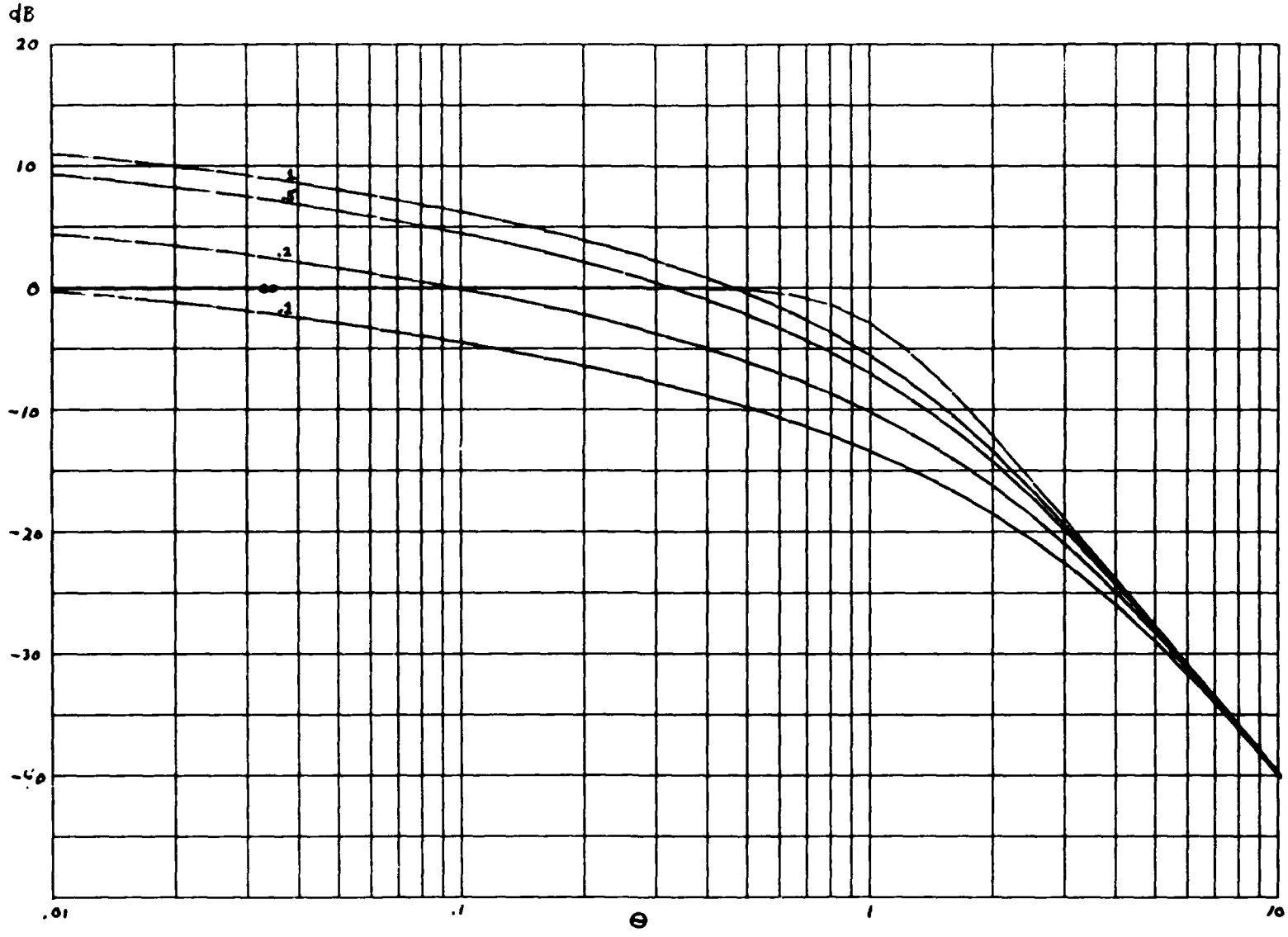

Fig. 4 - Beam Patterns $2\alpha L = 1$ to .01

Naval Underwater Systems Center
NP24 - 8771? - 12 - 75

Official Photograph

TM-230-75

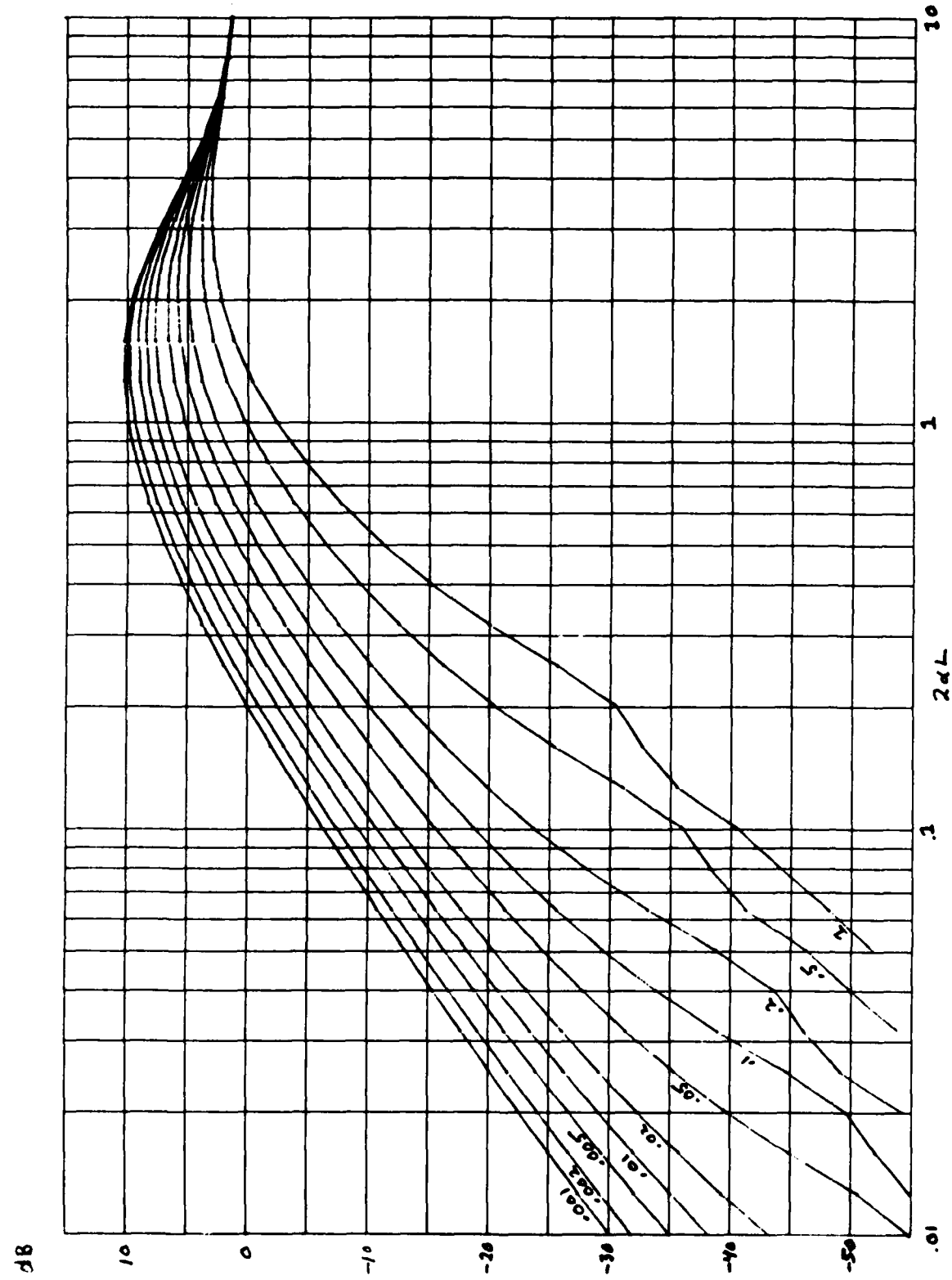

Fig. 5 - Source level relative to Westervelt vs. scaled distance. The parameter is the nearfield absorption number (plane wave model).

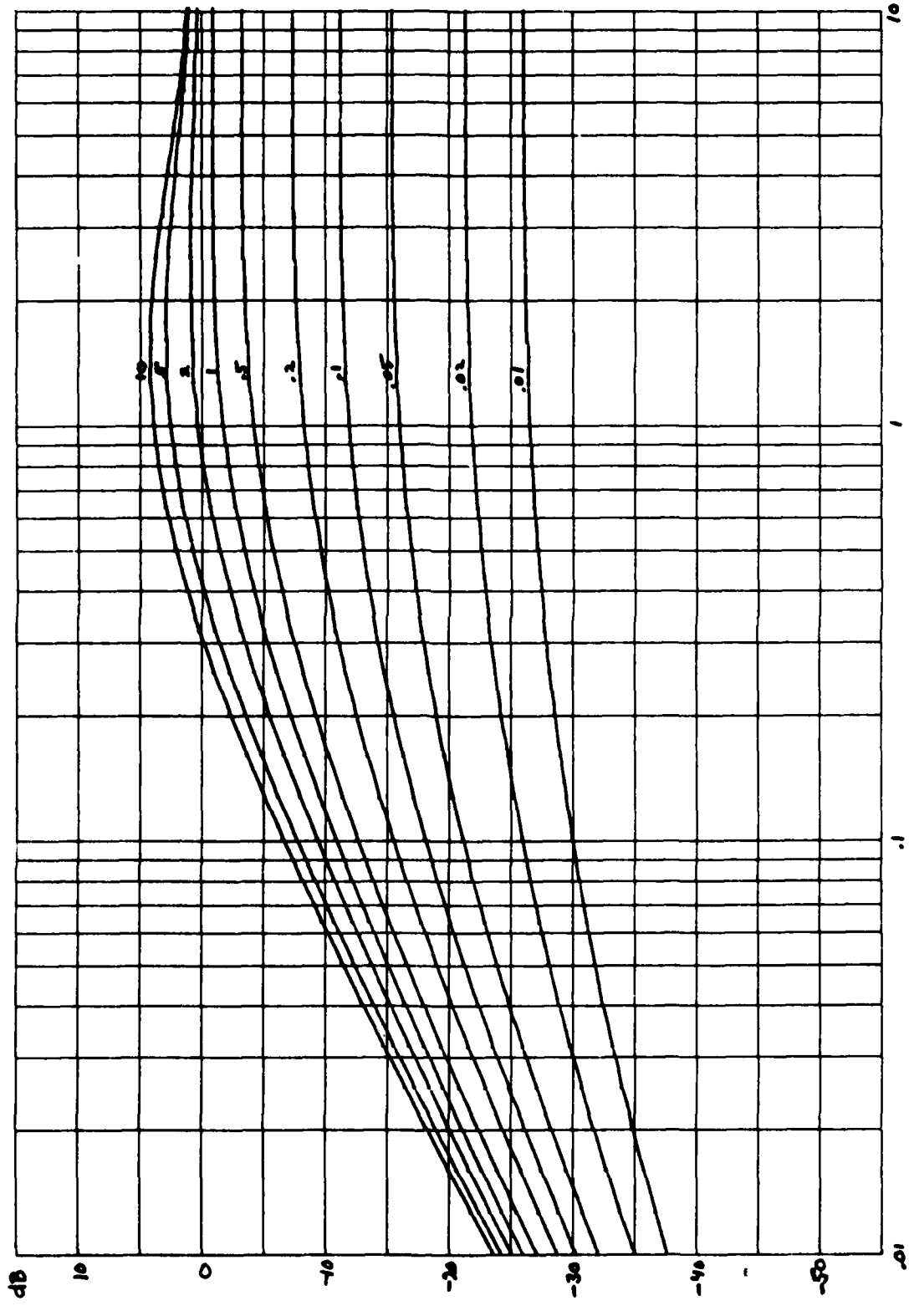

Fig. 6 - Source level relative to Westervelt vs. scaled distance. The parameter is the farfield absorption number (spherical wave model).

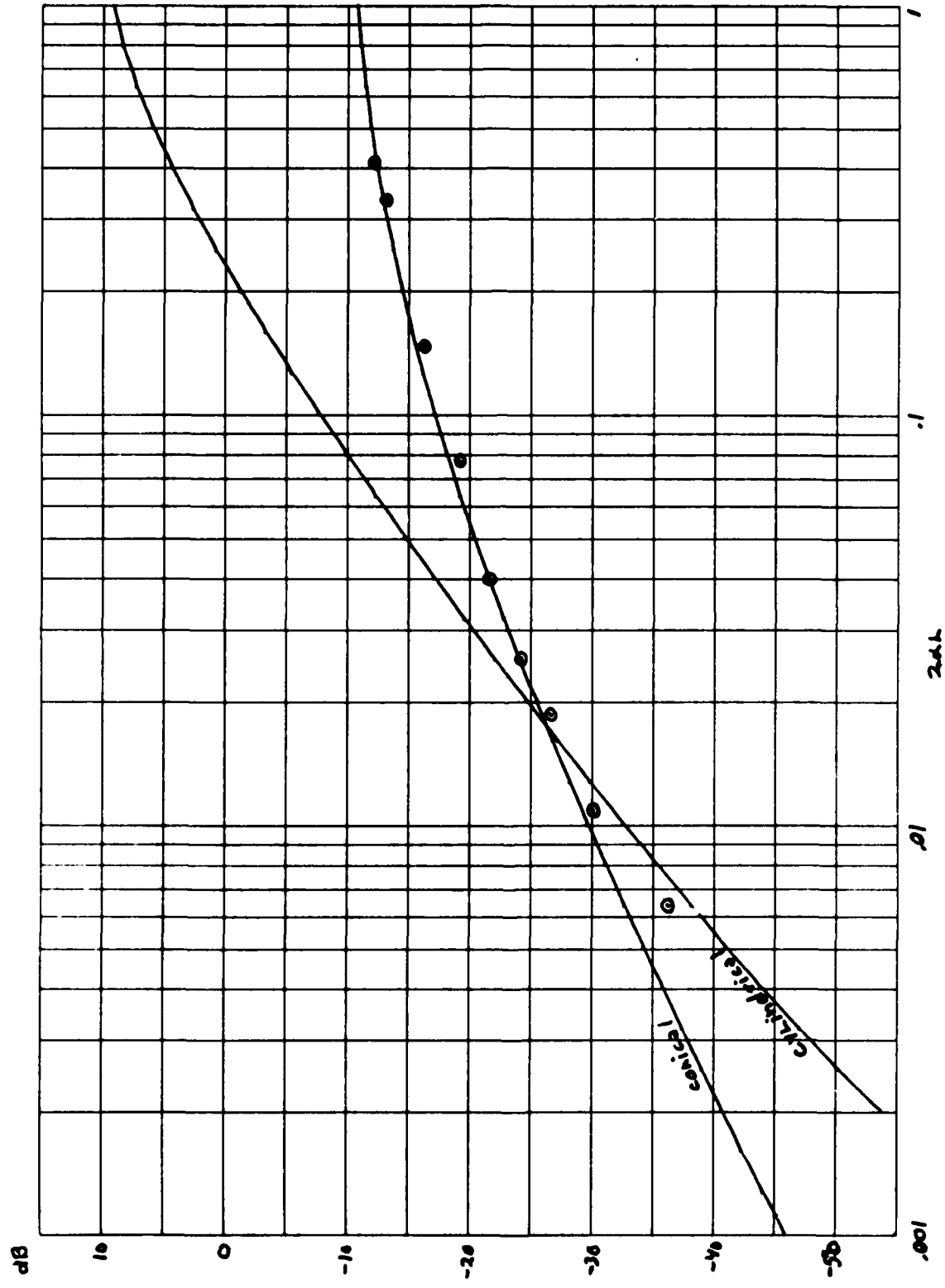

Fig. 7 - Comparison of predicted and experimental values of apparent source level vs. range $2\pi R_0 =$ 0.0175, $R_0/h = 7$

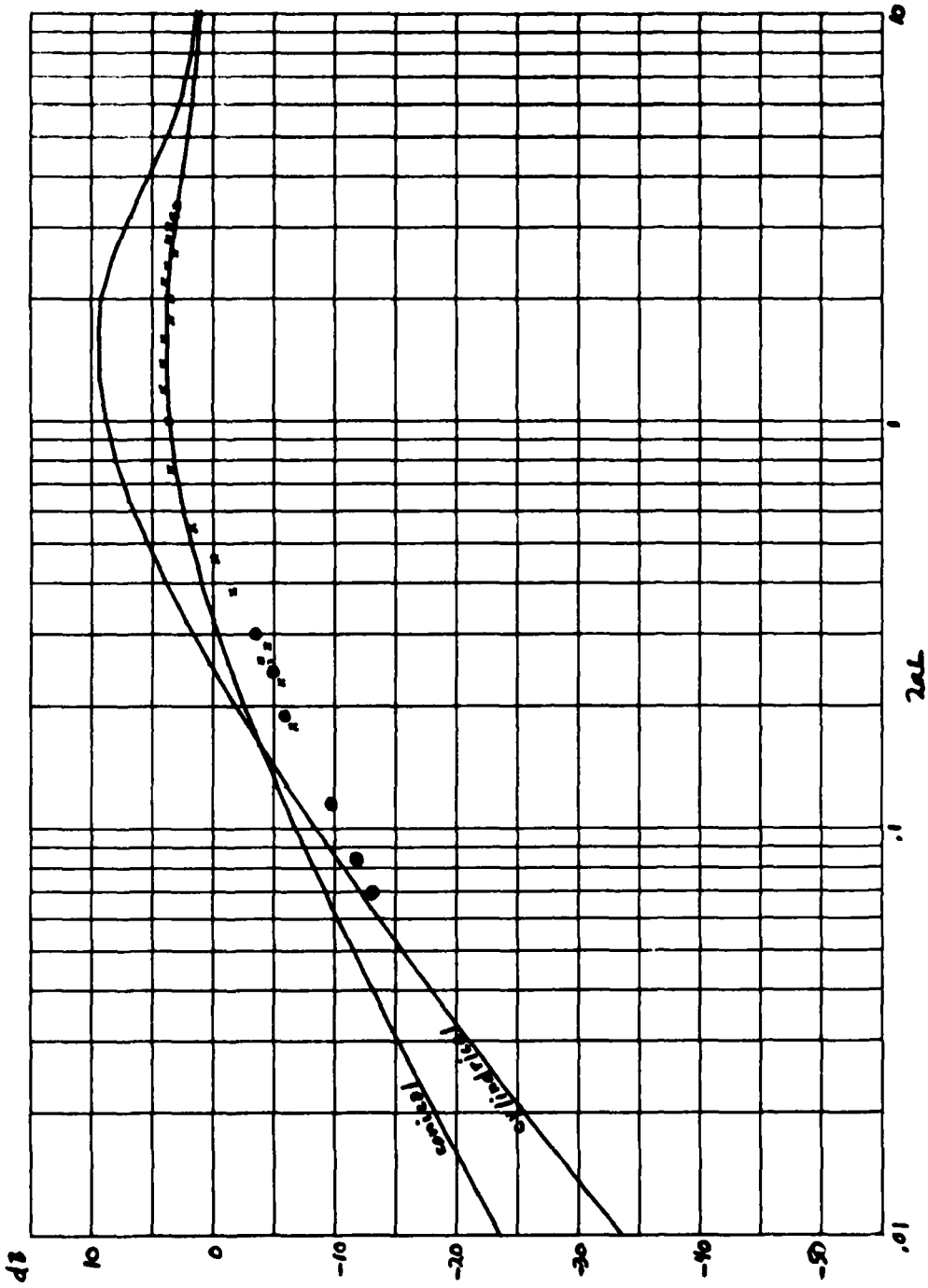

Fig. 8 - Comparison of predicted and experimental values of apparent source level vs. range $2\pi R_o = 0.17$, $k_o/k = 50$

Naval Underwater Systems Center
NE24 - 87672 - 11 - 75

Official Photograph

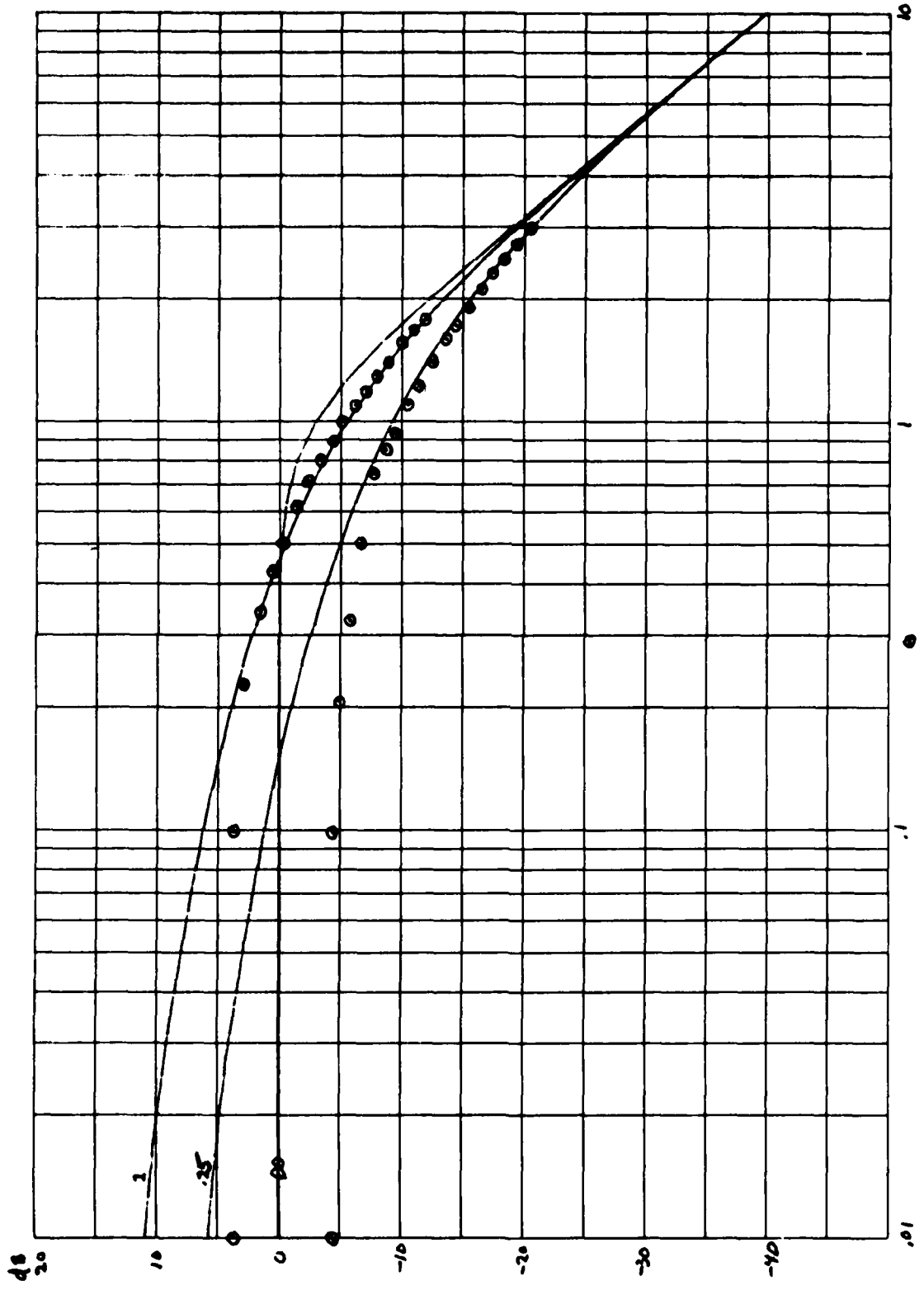

Fig. 9 - Comparison of predicted and experimental beam patterns $2\alpha L = 0.25$ and 1, $k_o/k = 50$

Official Photograph

Naval Underwater Systems Center

P24 - 57715 - 12 - 75